

# Recommender system in X inadvertently profiles ideological positions of users

Paul Bouchaud<sup>1,2,†</sup> & Pedro Ramaciotti<sup>1,2,3,‡</sup>

<sup>1</sup>Complex Systems Institute of Paris Ile-de-France CNRS, Paris, France.

<sup>2</sup>médialab, Sciences Po, Paris, France.

<sup>3</sup>Learning Planet Institute, CY Cergy Paris University, Paris, France.

† [paul.bouchaud@cnrs.fr](mailto:paul.bouchaud@cnrs.fr)

‡ [pedro.ramaciotti-morales@cnrs.fr](mailto:pedro.ramaciotti-morales@cnrs.fr)

## Abstract

Studies on recommendations in social media have mainly analyzed the quality of recommended items (e.g., their diversity or biases) and the impact of recommendation policies (e.g., in comparison with purely chronological policies). We use a data donation program, collecting more than 2.5 million friend recommendations made to 682 volunteers on X over a year, to study instead how real-world recommenders learn, represent and process political and social attributes of users inside the so-called *black boxes* of AI systems. Using publicly available knowledge on the architecture of the recommender, we inferred the positions of recommended users in its embedding space. Leveraging ideology scaling calibrated with political survey data, we analyzed the political position of users in our study (N=26,509 among volunteers and recommended contacts) among several attributes, including age and gender. Our results show that the platform’s recommender system produces a spatial ordering of users that is highly correlated with their Left-Right positions (Pearson  $\rho=0.887$ , p-value  $< 0.0001$ ), and that cannot be explained by socio-demographic attributes. These results open new possibilities for studying the interaction between human and AI systems. They also raise important questions linked to the legal definition of algorithmic profiling in data privacy regulation by blurring the line between active and passive profiling. We explore new constrained recommendation methods enabled by our results, limiting the political information in the recommender as a potential tool for privacy compliance capable of preserving recommendation relevance.

Can recommender systems on social media inadvertently learn and leverage political preference of users? The answer to this question is relevant to data privacy regulation, when internal representations made by recommenders may map to traditional forms of measurement (such as political survey data), and for the study of interactions between individuals and AI systems. Recent studies have shown that machine learning procedures can autonomously learn sensitive attributes (1), and that social media data can be leveraged in estimating individual political preferences (2), ideological positions (3), and stances on issues (4). This body of work has nurtured the expectation that any recommender system capable of serving relevant content on social platforms must, at least to some degree, capture and leverage political preferences among several other attributes on which personal preferences may hinge. At the same time, the massification of social media and its entanglement with politics have motivated a growing body of work focused on political polarization and segregation, not least because of the role and potential consequences of AI systems computing recommendations on these platforms (5). A better understanding of the mechanisms through which AI systems learn, represent, and leverage ideological orientations on online platforms presents significant implications for developing regulatory instruments and compliance tools, and for studying social systems interacting with AI ones.

Most works studying recommender systems and politics investigate recommended items (e.g., content or contacts) either i) analyzing recommendations by measuring properties such as diversity and biases (6–9), or ii) assessing the causal impact of recommendations through controlled experiments with different recommendation policies (10–12). Several studies have addressed the question of machine representations of ideology from data during training, but mainly of contents (as opposed to individual actors), focusing on a few actors (13) (e.g., political elites such as Members of Parliament, comparing machine representations with measures such as ideology scaling of parliamentary voting), or on limited experimental settings, as opposed to large real-world systems with large user bases (14). Fewer studies have addressed how recommender systems in social platforms learn, represent, and process political information on large numbers of regular users and contents when computing recommendations (15). The main challenges in gaining further insights into how these AI systems work are the difficulty in using AI explainability methods in these real-world settings, and in collecting exposure data (6, 7, 10, 11, 16).

In this work, we develop and validate a method to infer an approximation of the embedding that X's (previously Twitter) AI recommender system leverages in computing friend and content recommendations. X is a relevant platform for such a study because political figures actively use it (17) (making it a pervasive tool in elections (18)), because of its entanglement with the media sphere (19), and because

users cannot create private or semi-private communication spheres, casting a wide scope for recommendation. First, we collected more than 2.5 million real “Who to follow” friend recommendations shown on the platform via a browser plugin installed by 682 users during a data donation campaign, between January 2023 to May 2024 in France (a country with high percentage of usage of X, which is also covered by the EU's General Data Protection Regulation, GDPR, forbidding the processing of sensible data categories without consent, including data on political opinions), involving more than 26 thousand users. Second, we used publicly available knowledge about the platform's AI system architecture to infer an approximation of the embedding computed by X's recommender system pipeline and that drives recommendations on the platform (20). At its core, this AI system embeds users, posts, and advertisements in a high-dimensional space where inner product similarities are ranked to recommend these items to users (21). Using this explicit formulation of inner product and ranking operations, we propose and validate a method to infer the most probable embedding positions for all users in our study.

To examine the political attributes of users in this space, we rely on ideological scaling (22) of the follower network connecting them to political figures (3), which we calibrated using political survey data (4). We compute additional user attributes to inspect the embedding space, including estimated age and gender from users' profile text and photos (23), and their interests in various domains (e.g., news, sports, or science) based on the contents of their posts. Using these attributes we inspect the embedding space of the recommender in the platform to explain computation of recommendations in terms of these attributes. Specifically, we seek to establish the following facts. 1) That a spatial direction in the embedding of the recommender positions users in a way that is highly and significantly correlated with their Left-Right positions. 2) That this spatial direction is not significantly aligned with other direction in the embedding that position users according to other attributes relevant for recommendation. 3) That the positions of users on the direction along which positions are correlated with Left-Right leanings has an impact in the computation of recommendations.

The existence of political profiles inadvertently learned by AI systems raises important questions for regulation whenever these profiles can be shown to be sufficiently similar to traditional forms of profiling, such as those resulting from self-positioning ideology questions in survey research. Several data privacy regulations forbid the processing of data that reveal political opinion without explicit consent from users. In the context of the expectation that recommenders in digital platforms must learn, represent and leverage political opinions (among other traits) in some form, we provide the first quantifiable measurement of this phenomenon for a platform counting hundreds of millions of users worldwide. We show that X's recommender system produces a linear internal

representation of recommended contacts that correlates with their Left-Right leanings.

Our findings point to a growing inconsistency in the application of several data privacy regulations. Regulations in South Korea, Switzerland, Brazil, and the EU forbid the processing of political opinions without explicit consent, and newer EU regulations such as the Digital Services Act (DSA) build on previous data privacy ones. Our work suggests that the distinction between active and passive profiling may come into question when AI systems process data produced by large numbers of regular individuals and when AI explainability methods such as ours may make visible (to platforms, regulators, and regular users) how this processing maps to the treatment of uncontroversial definitions of political opinion data. Our work also has implications for research on AI mediation of digital socio-information systems. First, it provides a way to further investigate the dynamics of human-AI systems with regard to political opinion processes and information exposure. Second, it enables new recommendation policies and algorithm design tools resulting from explicitly modifying the machine representations of political attributes. We explore the latter by investigating the potential consequences of complying with data privacy regulation, constraining the ideological leanings in the spatial representation of individuals in the recommender of X, measuring changes in content relevance and diversity.

## Reconstructing the embedding space of the recommender in X

The “Who to follow” (WTF) recommendations (24) reportedly drive over one-eighth of all follower connections (25), and uses several algorithms to surface relevant accounts that are then ranked before recommending them (26). See Extended Figure S1 of the Supplementary Information document for an overview of the architecture of the service. X’s recommender system leverages explicit user signals—who they follow, repost (i.e., share), reply to, or click on—resulting in their representation in a multidimensional embedding space. Positions in this embedding space are then leveraged in computing similarities via inner product operations, producing candidates for recommendation which are then ranked and served to users. See Extended Figure S2 for an illustration of the data representation of entities that are embedded, according to X’s scientific publications (21). While the architecture and algorithms involved in the computation of this embedding are publicly known to some extent, the data used during training and the positions of entities in the embedding of the recommender are not. This poses a double problem for explainability: first because of the opacity of the model (i.e., the so-called “black box” problem), but also the lack of access to the model itself, which constitutes a major barrier for most independent scientific research on algorithmic

recommendation.

To collect data traces allowing us to infer their positions in the embedding space of the WTF service, we created a data donation program in which users could install a browser plug-in that relayed to us recommendations of friends and contents serviced to them by the platform. We advertised the browser plug-in on X and on local media outlets in the fall of 2022, offering volunteers who installed it a personalized analysis of their feed. No monetary incentive was offered to volunteers. From January 1st, 2023, to May 1st, 2024, we collected 2,549,008 personalized friend recommendations seen on the platform by 682 fully-compliant volunteers (set  $\mathcal{V}$ ) i.e., individuals who opted into the data collection program, used the browser extension for at least one month, visited X to see at least 30 contact recommendations, and did not opt out of the study by uninstalling the plug-in or by later requesting their data to be deleted from our database. From over 105K accounts recommended during the observation period, we retain 26,338 accounts that were recommended to two or more volunteers (set  $\mathcal{U}$ ) to define the population for our study as  $\mathcal{E} = \mathcal{U} \cup \mathcal{V}$  ( $|\mathcal{E}| = 26,509$ ), for which we have data related to recommendations.

Using the platform’s API, we also collected the follower network subtended by population  $\mathcal{E}$ , as well as profiles and posts produced by them. We cast the problem of approximating the positions of users in  $\mathcal{E}$  in the embedding of the recommender as an optimization problem for the prediction of observed recommendations, constrained to the known architecture of the embedding used by the WTF service (21). Following X’s own design, we consider a 256-dimensional embedding space (27) and we solved the optimization problem (namely, estimating the embeddings that best explained observed data) with a gradient descent algorithm. We assess the quality of the inferred positions in the embedding by evaluating the accuracy with which the resulting recommender can predict observed WTF recommendations in our study. Holding out 10% of our data (including both recommended and not recommended users), our trained model yields an AUC-ROC value of 0.700. For comparison, three baseline approaches—recommending random second neighbors, second neighbors with the highest number of followers, or second neighbors followed by the most first neighbors—all perform below chance level (AUC of 0.467, 0.425, and 0.423 respectively). The probability of a random baseline—predicting edges either uniformly or weighted by frequencies observed in the training dataset—to equal or outperform our trained model is less than  $10^{-5}$ .

When evaluating only positive test recommendations (i.e., friend recommendations observed in the study) against a pool of 100 randomly chosen non-recommended second-order friends, the model achieves a Precision@1 of 0.725 and a Precision@3 (the number of recommendations shown on the right-side panel on X) of 0.691.

We tested the robustness and reliability of the inferred po-

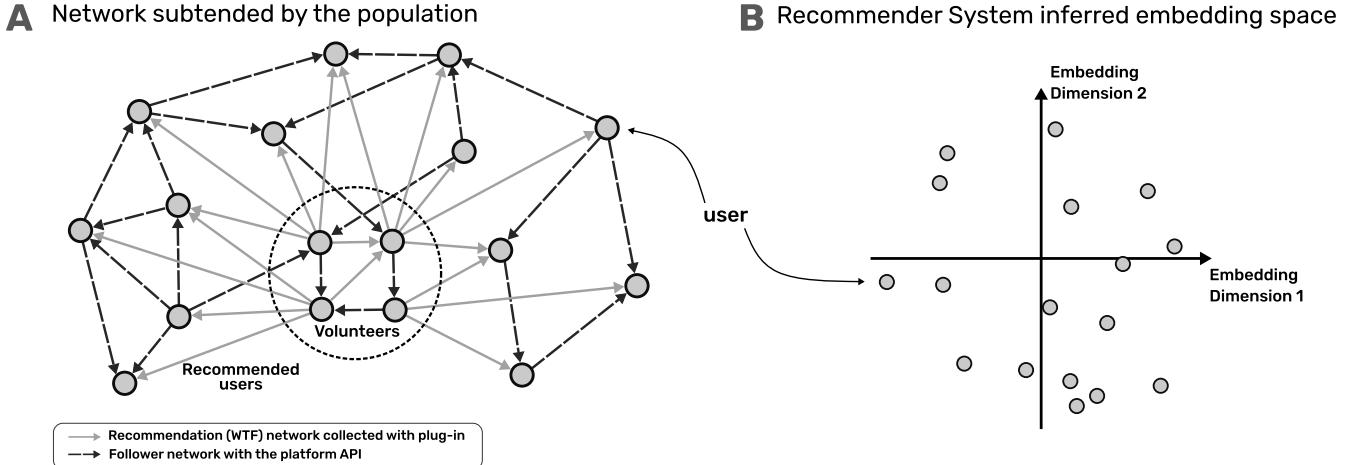


**Figure 1:** Schematic representation of the population of  $X$  users for the study and the inference of their position in the embedding space of  $X$ 's recommender system. (A) Population of the study (data volunteers  $\mathcal{V}$  and recommended users  $\mathcal{U}$ ) subtending networks for friend recommendation (in orange arrows) and following relations (in purple arrows), collected respectively with a data donation program using a browser plug-in and  $X$ 's API. (B) Schematic representation of the embedding space with every user  $i$  in the population  $\mathcal{E}$  having a position  $\phi_i$  in the 256-dimensional embedding.

sitions in the embedding for alternative training parameters and sub-sampling strategies simulating potential sources of biases, including: i) the possibility that volunteers saw recommendations on devices outside our study, ii) age, gender and ideological skews in our population, iii) changes in the activity and population of the platform during the period of observation (including changes around May 2023 related to change in platform ownership), iv) changes in the structure of the follower graph during the period of observation, and v) alternative parameters of the optimization problem. See the Methods section for a detailed description of the constrained optimization problem, its implementation, parametrization, validation and experiments demonstrating robustness and reliability.

## Inferring political and demographic attributes of users

To consider political attributes of users in our study, we rely on a dataset of users in  $X$  with inferred political positions on a Left-Right scale in 2023 (28). The authors of this dataset use multidimensional ideology scaling of follower networks on  $X$  (3, 29) and political survey data (30) for calibrating positions of large populations of users pooled from followers of Members of Parliament (4). The dataset includes a Left-Right scale calibrated to have three reference points: 0 (the leftmost position for political parties), 10 (the rightmost positions), and 5 standing as the political center. The dataset includes a second political dimension called anti-elite rhetoric, measuring attitudes towards elites and institutions, deemed by authors of the dataset as a second relevant dimen-

sion in the country of our study (France). 8,249 users in this dataset are also in population  $\mathcal{E}$  (i.e., 31.1%; see Figure 2.A). Extended Figure S14 & S15 show the positions of users in the dataset from (28) along the two dimensions and metrics assessing the quality of these calibrated positions.

We include additional user attributes in our study, both to control for potential covariates that might explain Left-Right positions of users encoded in the recommender system, and to further examine how these attributes are processed in the embedding space. To infer these attributes, we collected their profile bios (text and image), their followed accounts, and their last 200 published posts (either original or reposted), using the API of the platform. We infer the age and gender of users with the M3 model developed by Wang et al. (23), analyzing profile pictures, screen names, and biographies. The M3 model provides complementary probabilities (i.e., adding to 1) of being either “male” or “female”, allowing us to consider a Male-Female dimension ranging from the highest probability of being classified as male to the highest probability of being classified as female. The M3 model also provides complementary probabilities of being in age groups: 0-18, 19-29, 30-39, 40 and older (Extended Figures S11 & S12 show agreement of inferences using M3 by comparison with those achieved with other models and with attributes self-reported by volunteers).

We also consider the popularity of accounts, measured as the percentile rank of number of followers to account for long-tailed distributions (results are unchanged when considering the logarithm of the number of followers), and attributes capturing the interest that users have in different topics by computing a topic modeling classification of their last 200 posts, leveraging the model developed by Antypas et al. (31),

specifically designed for posts on (then) Twitter. Among these available topics, we specifically consider interest in news as a covariate that might explain political positions encoded by a recommender system.

Attributes in our population exhibit low absolute Spearman correlations (Figure 2.B), with the two highest being between age and interest in news ( $\rho = 0.339$ ; i.e., older users tend to exhibit more interest in news content) and between age and negative attitudes towards elites and institutions ( $\rho = -0.263$ ). Left-Right leaning (our main variable of interest) exhibits a lower absolute correlation with age ( $\rho = 0.128$ ) and gender ( $\rho = -0.079$ ). All the above-cited correlations have p-values  $< 0.001$ .

## Measuring attributes encoded by the recommender system

Next, we proceed to the identification and measurement of information on attributes of users that might be encoded in the embedding space. The main hypothesis behind this identification and measurement procedure is that these AI systems might develop representations that match relevant constructs, such as Left-Right ideological leanings. This expectation is motivated by the use of inner product similarities in ranking, based on positions on the embedding, on the part of the recommender.

To identify and measure the information of attributes of users encoded in the embedding, we leverage a search of spatial directions in this space and that induce high correlations with attributes, using Canonical Correlation Analysis (CCA), treating user embeddings as a multivariate dataset and inferred attributes as univariate ones. For each user attribute, a CCA identifies the spatial direction in the embedding space that maximizes correlation between the projected positions of users along the direction and the selected attribute. Because our goal to provide an explanation for the embedding on the semantic provided by attributes, we compute a CCA regression independently for each feature for interpretability. The CCA directions determined in this way, achieve Pearson correlations of different qualities for the selected attributes (see Figure 3.A; all correlations have p-value  $< 0.0001$ ): Left-Right leaning ( $\rho = 0.887$ ), anti-elite rhetoric ( $\rho = 0.863$ ), interest in news ( $\rho = 0.848$ ), popularity ( $\rho = 0.730$ ), age ( $\rho = 0.562$ ), and gender ( $\rho = 0.384$ ). Extended Table S2 shows all Pearson correlations achieved by directions identified with the CCA for political and demographic attributes, as well as for attributes regarding interests in topics, and platform activity metrics. These inferred CCA directions represent the best possible linear encoding of the attributes of users learned and represented by the recommender system.

To further validate that these directions produce a reliable ordering of users by the value of their attributes, we assessed the quality of their positions projected onto these di-

rections, for Left-Right leaning ( $\mathbf{w}_{LR}$ ), for anti-elite rhetoric ( $\mathbf{w}_{AntiElite}$ ), for age ( $\mathbf{w}_{age}$ ), for gender ( $\mathbf{w}_{gender}$ ), for interest in news ( $\mathbf{w}_{News}$ ), and for popularity ( $\mathbf{w}_{pop}$ ). We assess the spatial ordering of users that follow Members of Parliament of parties with clear ideological leaning (using a Mann-Whitney U test): the center-leaning party *Renaissance* (RE), the Right-leaning party *Rassemblement National* (RN), and the Left-leaning party *La France Insoumise* (FI) (obtaining respectively 27.85%, 23.15% and 21.95% of the vote in the last presidential elections in 2022, followed by a fourth candidate obtaining 7.07% of the vote). Direction  $\mathbf{w}_{LR}$  induces an order (Extended Figure S19) of users such that followers of MPs from FI are to the left of those of the followers of MPs from RE ( $p < 0.0001$ ), which are to the left of those of the followers of MPs from RN ( $p < 0.0001$ ). Direction  $\mathbf{w}_{AntiElite}$  also induces an order of users (Extended Figure S20) such that followers of MPs from FI and RN (widely regarded as anti-elite parties (32)) are positioned to the right (i.e., displaying stronger anti-elite rhetoric) of followers of MPs from RE ( $p < 0.0001$ ).

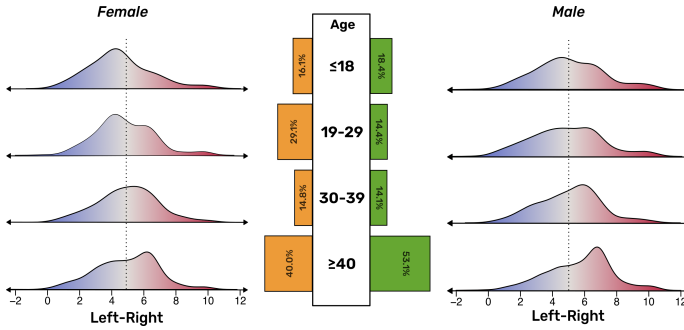
Measured by a Mann-Whitney U test,  $\mathbf{w}_{gender}$  orders users classified male or female ( $p < 0.0001$ ), and  $\mathbf{w}_{age}$  produces a relative pair-wise ordering of age groups ( $p < 0.0001$ ). Classification of users into age and gender groups is performed at a 0.5 probability threshold on the results of the M3 model. To further validate positions along these CCA directions, we computed the accounts followed, and the words and hashtags used by users at their extremes, and showed in the Methods section how they relate to corresponding ideological leaning, demographic group, or topic of interest.

## Measuring the alignment between attributes encoded in the embedding space

Is the Left-Right spatial representation of users learned by the recommender system different from the representation of age or gender? To assess the similarity and alignment between positions of users along the inferred attribute directions in the embedding space, we inspect two metrics: 1) the cosine similarity (ranging from -1 to 1, with 0 meaning orthogonality) between each pair of CCA directions, and 2) the correlation between the positions of users along each pair of CCA directions capturing user attributes in the embedding space of the recommender.

CCA directions do not display a high degree of spatial alignment when measured via cosine similarity (see Figure 3.B). The highest (absolute) values for cosine similarity are between age and interest in news (0.304), and age and gender (-0.229), followed by the alignment between popularity and gender (-0.168). Only one pair of CCA directions displays a statistically significant alignment (at  $\alpha = 0.01$ ) measured by the cosine similarity: age and interest in news. We measure the p-value as the proportion of randomized co-

### A Demographic and political profile of the population



### B Correlation between features in the population

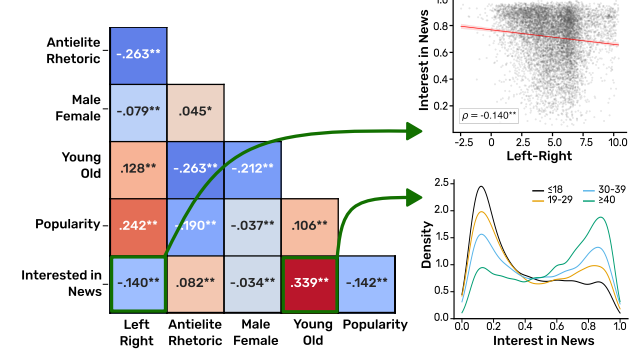


**Figure 2:** Characterization of the population in the study. (A) Distribution of Left-Right ideological leaning of X users segmented by age and gender. (B) Pairwise Spearman correlations between the inferred attributes of users (\* indicates  $p$ -value  $< 0.01$ , \*\* indicates  $p$ -value  $< 0.001$ ). The correlation between Left-Right leaning and degree of interest in news is  $-0.14^{**}$ . The density plots for the degree of interest in news of users in different age groups illustrates a comparatively higher correlation between this attribute and age.

sine similarities (i.e., permuting the attributes of users) that exceed the observed similarity between two CCA directions.

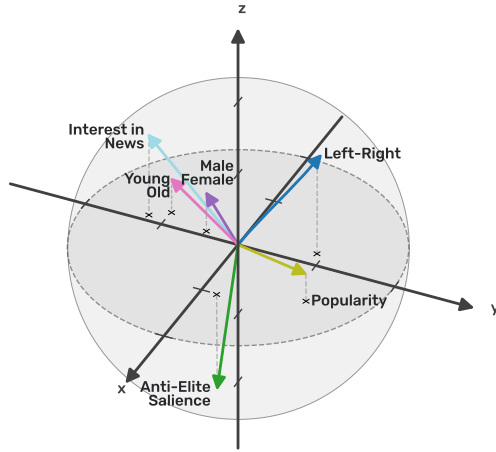
A measurement of the Spearman correlation between positions of users projected onto the CCA dimensions reveals different degrees of similarity among them. The three highest (absolute) correlations observed (all with  $p$ -value  $< 0.001$ ) are for positions projected onto CCA directions:  $\mathbf{w}_{age}$  and  $\mathbf{w}_{news}$  ( $\rho = 0.620$ ),  $\mathbf{w}_{age}$  and  $\mathbf{w}_{Anti-elite}$  ( $\rho = -0.524$ ), and  $\mathbf{w}_{Popularity}$  and  $\mathbf{w}_{LR}$  ( $\rho = 0.404$ ). Importantly, Left-Right leanings in the recommender (captured by  $\mathbf{w}_{LR}$ ) do not induce high correlations with machine representations of age (as captured by  $\mathbf{w}_{age}$ ;  $\rho = 0.172$ ) nor gender (as captured by  $\mathbf{w}_{age}$ ;  $\rho = -0.275$ ) (see Extended Figure S30 for the spatial distribution along these pairs of directions). Extended Figure S29 shows the values of Spearman correlation between positions along all CCA directions.

These results show that the information linearly encoded by the recommender along spatial directions identified with CCA, are largely orthogonal. An attribute of special interest for both the study of online politics and data privacy regulation are Left-Right leanings. Direction  $\mathbf{w}_{LR}$  that arranges users by Left-Right ideological leaning, induces projected positions that cannot be predicted with high accuracy by leveraging positions of users along other CCA directions capturing other attributes. In other words, up to linear encoding of attributes in the embedding of the recommender, information on ideological Left-Right leaning is nearly orthogonal from other attributes. While more complex geometrical models of encoded information on attributes might possibly be more explicative (e.g., nonlinear manifolds), our results show that, even considering a linear encoding, the recommender system can be proven to store information on the ideological leaning of users.

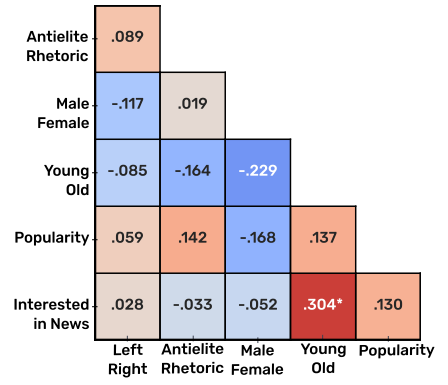
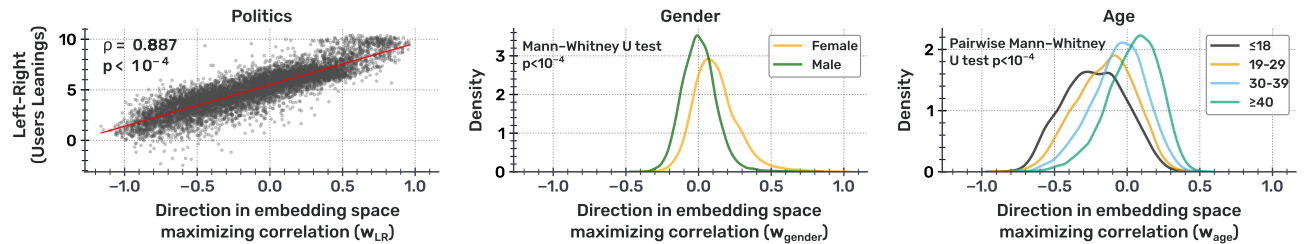
## Constraining political profiling in recommendations

Even though political attribute processing was not specified in the design objectives of this AI system, our findings show that it does engage in such processing according to definitions contained in several data privacy regulations (e.g., EU’s GDPR forbids non-consenting processing that “reveals” political opinions). Our findings also point to potential ways in which this can be mitigated, by constraining the amount of information on political leanings of users that can be used in the computation of recommendations. The proposed procedure consists in computing the subspace in the embedding that is orthogonal to  $\mathbf{w}_{LR}$  (i.e., a 255-dimensional hyper-plane in the embedding space), and projecting all recommendable entities onto it before using inner products in the resulting space to assess similarities and formulate recommendations (Figure 4.A). In the scope of our study, we propose an experiment recommending users on  $\mathcal{E}$  to investigate the effects of such a procedure. The new embedding resulting from this procedure is *protected* (34) from having linearly encoded information about ideological leanings of users.

This proposed procedure holds resemblance to that described as “debiasing” of language models by Bolukbasi et al. (35), which allows zeroing-out the components of neutral words in the direction of a “gender subspace” (in their work) to mitigate gender stereotypes in word embeddings. As shown by Gonen and Goldberg (36) and by Ravfogel et al. (34), linearly-encoded attributes in high-dimensional spaces might be encoded in several orthogonal dimensions. This means that, even after projecting positions of users in the embedding onto the subspace that is orthogonal to  $\mathbf{w}_{LR}$ , in the new resulting embedding, it might be possible to find a second dimension that also encodes (with lower induced absolute correlation) ideological leanings. Therefore, as Rav-

**A** Directions in the embedding space correlated with attributes

Population Attributes	Best Correlation in Embedding
Left-Right	0.887
Anti-Elite Salience	0.863
Male-Female	0.384
Young-Old	0.562
Popularity	0.730
Interest in News	0.848

**B** Cosine similarities between correlated directions**C** Comparing population attributes with projection onto correlated direction in the embedding space

**Figure 3:** (A) Three-dimensional representation of directions in the 256-dimensional embedding space of the recommender system that maximize the correlation with attributes of users, identified using Canonical Correlation Analysis (CCA). The three-dimensional visualization was obtained through a Locally Preserving Projection (33). Vector norms of directions associated with attributes correspond to absolute correlations with these attributes, reported in the adjacent table (all  $p$ -values  $< 0.0001$ ). (B) Absolute cosine similarity computed in the 256-dimensional embedding space between directions in the embedding space identified with CCA and that maximize correlations with attributes of users (\* indicates  $p$ -value  $< 0.01$ ). (C) Comparison of attributes of users along the CCA directions in the embedding that maximize correlations with three features: Left-Right leaning  $w_{LR}$ , age  $w_{age}$ , and gender  $w_{gender}$ .

fogel et al. (34), we repeat the identification and projection procedures, iteratively computing a CCA identification of directions encoding Left-Right leanings, until no subsequent identifications yield statistically-significant correlations (set at  $\alpha=0.01$ ). This means that we iteratively remove linearly-encoded ideological information by projecting into new subspaces, until the p-value of the maximal correlation identified with CCA overflows above 0.01.

To evaluate the effect of our procedure we compare recommendations computed using X’s described pipeline based on embeddings (21), using both the original embedding and the new protected embedding void of linearly-encoded ideological leanings. We formulate 50 friend recommendations for each user and evaluate i) the Left-Right ideological diversity of recommended profiles (measured as the standard deviation of Left-Right positions) and ii) recommendation relevance. To assess relevance, we compare, through cosine similarity, the topic distributions of posts shared by friends suggested using the original embeddings versus those suggested using the protected embeddings. Additionally, we specifically examine the interest in news and politics among users suggested by the original versus protected embeddings, where interest is quantified as the proportion of each user’s last 200 posts classified as discussing news using the model by Antypas et al. (31). By selectively removing information that linearly encodes users’ Left-Right ideological leanings, we observe an increase of the Left-Right political diversity of recommendations (Cohen’s  $d = 0.477$ , 95% CI [0.459, 0.495] using the original embeddings as control. Confidence intervals were determined through user-level bootstrapping.) while maintaining relevance, as shown in Figure 4.B. Specifically, the intervention preserves the topics shared by suggested friends—the cosine similarity of topic distributions between friends suggested by protected and original embeddings is 0.948 (95% CI [0.751, 0.999])—and maintains similar interest in news between recommendation recipients and recommended friends (Cohen’s  $d = -0.009$ , 95% CI [-0.032, 0.014]).

In summary, our procedure demonstrates that linearly-encoded ideological profiles can be removed in our setting without significantly compromising (at least in the setting of our study) recommendation relevance, as measured by topic-specific metrics. However, the impact on recommendation diversity is significant. Section G.4 of the Supplementary Information examines the effects of our procedure applied to other attributes, showing that Left-Right leanings encoded in  $w_{LR}$  is the attribute that, when removed, leads to the most significant change in the set of recommended contacts. Recent literature reports mixed effects of diversified recommendations on political polarization, with some evidence suggesting potential exacerbation of affective polarization (37). These potentially adverse effects remain poorly understood across different national contexts and at varying levels of diversity intervention.

## Discussion and conclusions

Our results show the recommender system in X inadvertently learns political orientations of users, meaning that these orientations are stored in the representation space of this AI system computing recommendations and that these orientations have an impact in the computation of recommendations. The encoding of information of political preferences may occur without users volunteering this information, without the encoding being part of the design of the recommender, and unbeknownst to platforms. This possibility has been recently suggested in previous works (15), and our results provide the first empirical evidence for real-world AI systems in a social media platform serving content to large numbers of users, in which AI data processing occurs at the unit of individuals (as opposed to only at the level of contents or posts), and for large numbers of regular individuals. We show that additional spatial directions encode other fundamental socio-demographic and thematic attributes, these directions being largely independent (i.e., not aligned in the embedding space). Our demographic and political geometry of a real-world recommender system representation also provides the first concrete example of the linear representation hypothesis (38–40) in an AI system serving hundreds of millions of users worldwide.

Our exposure data comes exclusively from feeds displayed on browsers. Our study does not account for differences, both in the specificity of the recommender and in the behavior of users, between navigation in the browser and through X’s telephone app.

We present additional experiments in the Methods section demonstrating the limited effects of this potential bias source, and explore alternative cohort compositions and embedding training strategies in Supplementary Information. Additionally, embedding reconstruction is largely informed by the follower network structure, whereas X’s recommendations incorporate additional signals such as user actions on posts (41) (e.g., liking and sharing). Yet, these limitations do not undermine our central conclusion: if selected subsets of input signals enable the recommender to learn ideological representations of users, the overall system retains this capability, at least locally. While additional signals may enable more sophisticated models, the system fundamentally possesses the capacity to learn ideological representations from specific input components. Similarly, parts of the recommender system architecture cannot be included in our study, such as the heuristics that modify recommendations after inner product similarity ranking, and that include diversification, moderation, content balancing, and content proofing (26). However, if the recommendations that we observe in our study still contain the measurable traces of spatial representations of political preferences in the embedding space (despite these post-ranking heuristics), the system as a whole holds again the property of being able to inadvertently learn political positions of users. Future research may leverage

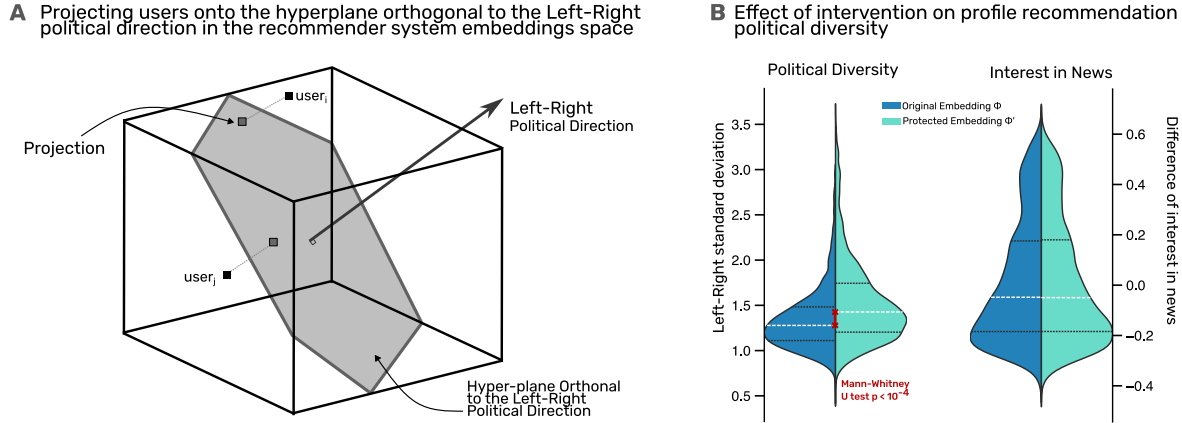


**Figure 4:** Constraining user recommendations from leveraging left-right political information. (A) Diagram of the intervention procedure. After identifying the direction in the latent space that maximally correlates with users' left-right political leaning, we iteratively project user representations onto the orthogonal subspace. (B) Effects on recommendations of constraining political information in the embedding of the recommender systems. For each user in the population, we compute 50 friend recommendations before (in blue) and after (in green) the intervention and compute the impact the distribution of the ideological diversity of recommendations as the standard deviation on the Left-Right scale, and the relevance as the similarity in interest in news between recipient of recommendations and recommended friends.

public knowledge on other components of the recommender system, such as the content-based components. Building on our results, future studies might also address whether recommender systems learning of political preferences persists across different languages, national settings, platforms, time periods, and services.

Our results have relevant consequences for platform and data privacy regulation. Several data privacy regulations worldwide prohibit the processing of sensitive personal data, including political opinions, without explicit consent given by users (e.g., European GDPR Article 9.1, Brazilian LGPD Article 11, South Korean PIPA Article 23, Swiss nFADP Article 5, thus pertaining to the rights hundreds of millions of individuals globally). Our results show that social media platforms might inadvertently create and process political profiles as defined by several regulations by simply “revealing” (e.g., EU’s GDPR in Article 9) political opinions and using them in the computation of recommendations, even under uncontroversial definitions such as processing representations of Left-Right leaning for large user populations in scales of political survey instruments. Legal scholars have previously considered this possibility (42, 43), in which biases might be neither in the training data nor in the design of an AI system, but “autonomously developed by the algorithm” (44). Our results provide the first empirical evidence of this possibility. Our results show that user attributes are encoded in approximately orthogonal directions in the embedding space (only age and interest in news show statistically significant alignment) in a recommender system that ranks based on inner product similarity. Our method makes implicit computation of ideological leanings explicit, creating a challenge for privacy regulation by blurring the distinction between active

and passive profiling. If these inadvertently developed profiles fall within the scope of regulation, regulators must define thresholds for what constitutes political opinion—potentially making numerous AI systems non-compliant. If, on the other hand, these profiles fall outside regulatory scope, platforms could exploit AI explainability tools to target users based on political profiles while remaining compliant, effectively nullifying privacy protections in cases like political ad targeting. Even assuming high alignment between sensitive and non-protected attributes in the embedding, contradictions persist. If platforms can legitimately infer sensitive attributes through aligned non-protected attributes, made explicit through a method such as ours, they can select proxy attributes correlated with political positions, undermining regulatory intent. If, on the other hand, sensitive attributes must never be processed regardless of alignment with other attributes, definitions of what constitute political opinion offered by regulators may risk prohibiting several common machine learning practices.

Finally, our work also points to ways in which social platforms and AI operators might seek to mitigate these risks, by developing constrained recommendation policies—i.e., recommendations computed using embeddings in which information about a sensitive attribute has been removed. Our experiments suggest that constraining the political information available for computing recommendations, their relevance is marginally affected, while increasing the political diversity of recommendations.

## Materials and Methods

### Recommendation and survey data collected via browser plug-in

To collect recommendations on X, we created a browser plug-in (also called a browser extension) that unobtrusively collects “Who To Follow” (WTF) recommendations displayed to volunteer users that installed the extension. We recruited participants following a call for participation launched on mainstream media coverage (newspapers and radio) and on Twitter advertising in the fall of 2022. The study incentivized participation by offering volunteers personalized analytics on their Twitter feed’s political diversity. No monetary incentives were offered to participants. Participants provided informed consent after receiving detailed information about the study objectives and data collection scope. Upon installation of the plug-in, users were asked their gender, their age group, their self-assessed ideological positions on a 11 point scale, and the devices from which they connect to Twitter. See Section B.2.1 for additional details on the recruitment strategy, attrition, and the questions used in this brief survey. Survey responses are only used in our study to validate the inference of socio-demographic and ideological attributes. Because extensive literature has demonstrated the potential sources of biases involved in data donation (45–47), we conducted an assessment of these biases in user attributes in Section D, and an assessment of the impact of these biases on our main results in Section C.2.3 (in experiments with different population compositions) of the Supplementary Information.

From January 1st, 2023 to May 1st, 2024, we gathered over 2,549,008 WTF friend recommendations displayed to 682 unique to volunteers during the period, henceforth referred to as set  $\mathcal{V}$ . We retained only users who saw at least 30 Who To Follow recommendations and did not opt out of the experiment or request data removal after providing consent. We report in Supplementary Information demographic statistics of our cohort. Extended Figure S4 shows the daily rate of collection of recommendations from users that used our browser plug-in. Participation and frequency of use by volunteers fluctuated during the observation period. We observe an increase in participation around the time of policy changes in the platform linked with changing ownership.

Within the more than 2.5 million WTF recommendations collected, we observed over 105k unique accounts that were recommended, with a highly skewed distribution (see Extended Figure S5 and Extended Table S1 showing the most recommended accounts). 26,338 unique accounts were recommended to at least two volunteers. We will refer hereinafter to this set of users as  $\mathcal{U}$ , and we define  $\mathcal{E} = \mathcal{U} \cup \mathcal{V}$  (users for which we have recommendation data) as the base population for our study, with  $|\mathcal{E}| = 26,509$ .

### User data collected via the API of X

Additionally, we used the API access of X to collect data on users in  $\mathcal{E}$ , including: their friends or followed accounts (allowing us to establish the follower network subtended by  $\mathcal{E}$ ), the last 200 posts they produced (including reposts), and information from their profiles, including text bio description, name and photo.

### Inferred positions of users in the embedding space

The WTF service employs precomputed high-dimensional representations of candidate users as user features (26). X described in scientific articles how Heterogeneous Information Network (HIN) embedding was used to formulate personalized recommendations (21, 27). X’s HIN consists of various entities, such as users or posts, being linked through relationships such as “likes”, “authorship” or “follow” (see Extended Figure S2.A). From observed relationships, X positions entities and relations within an embedding space that is used in downstream tasks to compute rankings of potential entities to recommend.

We used the data collected for this study and publicly available knowledge on the architecture of the recommender and its training procedure (21) to define the problem of inferring the positions  $\phi_i$  of users  $u_i \in \mathcal{E}$  in the embedding space used by X’s WTF service. We define this problem as that of estimating the positions of users in the embedding that yield the highest probability of computing recommendations that have been proposed by X to users on the platform, and captured by our browser extension.

We consider the edges  $e$  that link a user  $u_s$  (recipient of recommendations, the *source* of the link), with all potential other users  $u_t$  (the *targets* of the link and that might be recommended to  $u_s$ ). Embeddings of entities and links are related to similarities used in ranking through a scoring function  $f(e) = f(\phi_s, \phi_r, \phi_t)$  for an edge  $e$  of type  $r$  (in our case “Follow” and “WTF” relations) in the HIN connecting source entity  $s$  to target entity  $t$ . The model optimizes entities’ embeddings ( $\phi_s$ ,  $\phi_t$ , and  $\phi_r$ ) by maximizing the log-likelihood  $\log \sigma(f(e))$  (with  $\sigma$  being the logistic sigmoid function) for observed edges while minimizing it for unobserved ones (i.e., relations that do not exist in the data). In (21, 27), X reports adopting the *TransE* (for *translating embeddings*) scoring function defined as the sum of inner products:  $f(e) = f(s, r, t) = (\phi_s + \phi_r)^T \phi_t$ .

To infer the positions of users from  $\mathcal{E}$ , we leverage the data available for inference (WTF recommendations and the follower network; see Extended Figure S2.B), and cast the problem as an optimization constrained to the system architecture described in X’s scientific publications (21, 27). Specifically, we consider the loss function prescribed by X for the training of the embedding on HIN data, and train

the embedding that minimizes loss for our WTF and follower network data. In a successfully trained model, the inner product between a target account’s embedding  $\phi_t$  and, for instance, the sum of a source account’s embedding and the “Follow” relationship embedding ( $\phi_s + \phi_{\text{Follow}}$ ) should yield high values for actual follower relationships and low values otherwise. To infer embeddings  $\phi$  for users, we consider a convex combination of both relationships through the following loss function  $\mathcal{L}$ :

$$\mathcal{L} = \alpha \mathcal{L}_{\text{WTF}} + (1 - \alpha) \mathcal{L}_{\text{Follow}}, \quad (1)$$

where each relationship-specific loss component is defined as:

$$\mathcal{L}_r = \sum_{e \in \mathcal{P}_r} \log \sigma(f(e)) + \sum_{e' \in \mathcal{N}_r} \log \sigma(-f(e')). \quad (2)$$

$\mathcal{P}_r$  and  $\mathcal{N}_r$  denote the sets of positive and negative (i.e., not observed in our data) edges for a relationship type  $r \in \{\text{“Follow”}, \text{“WTF”}\}$ . Our formulation allows us to consider the inference of the positions of users embedding space by using only observed recommendations (i.e., setting  $\alpha = 1$ ), but also exploring improvements on the inference by integrating knowledge on the architecture of the embedding, using subsets of the signals that the WTF use during training (i.e., follower networks, setting  $\alpha < 1$ ).

## Sampling of negative edges for the inference

Combining our two datasets, we obtain the set of positive edges for the “Follow” and “Who to Follow” relationships, resulting in  $|\mathcal{P}_{\text{Follow}}| = 4,441,670$  “Follow” edges and  $|\mathcal{P}_{\text{WTF}}| = 110,164$  “Who to Follow” edges. As third party, we lacked access to the exact set of candidate accounts scored by X’s algorithmic systems, from which the “Who to Follow” list is computed after ranking, we then relied on sampling of negative edges, i.e., edges  $e$  that are not observed in the data. Specifically, we generated negative edges by corrupting positive ones, replacing target accounts with randomly sampled accounts. This sampling strategy is aligned with the default setting of PyTorch-BigGraph, developed by Meta (48) and used by X in (21), and includes (in equal proportion):

- **Uniform sampling:** target users are randomly selected from the entire pool of accounts with equal probability;
- **Prevalence-based sampling:** target users are sampled with probability proportional to their frequency in the positive edge set, reflecting their natural occurrence in the recommendations;

- **Second-neighborhood sampling:** target users are selected from friends of friends, i.e. being two hops away in the user-to-user network, capturing the local network structure.

Both uniform and prevalence-based sampling present disadvantages when used separately. Uniform sampling risks creating a model that learns to score edges primarily based on source and target node frequency rather than meaningful relationships between nodes. Prevalence-based sampling may not sufficiently penalize high scores assigned to rare entities. We corroborate the robustness of the trained embeddings to alternative negative sampling strategies in the SI in Section C.2.2. To further emulate X’s WTF pipeline, we include non-recommended second-order friends (26); excluding first-degree connections i.e. direct friends. The homophilic nature of X/Twitter networks (49, 50) motivates the search for new ties from friends of friends rather than random strangers. In our data, 62.4% of observed WTF recommendations are second-degree neighbors. Among recommended second neighbors, only 15.8% are followed by only one of the user’s friends, while half are already followed by at least 8 friends of the user to which recommendations are being proposed. The degree distribution (see Extended Figure S7) showcases that recommended second-degree neighbors tend to have substantially more first-degree friend connections compared to non-recommended ones. Consequently, prevalence sampling from non-recommended second-order friends provides particularly valuable negative examples, as these represent plausible but ultimately non-recommended connections —effectively serving as “hard negatives” for the model. Finally, in curating sets of negative WTF ( $\mathcal{N}_{\text{WTF}}$ ) and “Follow” ( $\mathcal{N}_{\text{Follow}}$ ) edges, we adopt a negative-to-positive ratio of 3:1, comparable with other works (51), resulting in  $|\mathcal{N}_{\text{Follow}}| = 3|\mathcal{P}_{\text{Follow}}|$  and  $|\mathcal{N}_{\text{WTF}}| = 3|\mathcal{P}_{\text{WTF}}|$ .

## Computing the inference of positions in the embedding

Following X’s implementation (27), we train a 256-dimensional embedding for users and relationship minimizing loss function in (1). The embedding was Glorot initialized (52) to prevent vanishing or exploding gradients during training, and optimized with Adagrad (53). We randomly segmented the curated edge set into 80%, 10%, and 10% splits for training, hyperparameter tuning, and final evaluation. The splitting was performed independently for each relation type of edge to maintain consistent Follow/WTF ratios across all sets.

We tuned the hyperparameter  $\alpha \in [0, 1]$  in (1) on a 10% holdout validation dataset. Due to the nondeterministic nature of stochastic gradient descent, we trained the model ten times for each  $\alpha$  value over three epochs, evaluating the ROC AUC on the validation dataset for each replicate (see Extended Figure S8). The model that best predicted

the relations in our dataset was achieved at  $\alpha = 62.6\%$ , yielding an AUC-ROC of  $0.7562 \pm 0.0018$  (standard deviation over ten replicates). Training the model solely on WTF ( $\alpha = 1$ ) or Follow ( $\alpha = 0$ ) data would have yielded AUC ROC values below 0.65 (Extended Figure S8). In what follows, we consider the embedding positions of the model trained with the optimal value  $\alpha = 62.6\%$  (assigning each “Who to Follow” training edge 1.67 times the weight of each “Follow” edge) over eight epochs, and three independent runs.

## Validating inferred positions in the embedding space

We inferred  $\Phi \in \mathbb{R}^{|\mathcal{E}| \times 256}$ , the positions of users from  $\mathcal{E}$  in the embedding, along with “Who to Follow”  $\phi_{\text{WTF}}$  and “Follow”  $\phi_{\text{Follow}}$  relationships embeddings. On a 10% held-out test set, the learned embeddings achieve an AUC-ROC of 70.0% for predicting “Who to Follow” recommendations when using non-recommended second-order friends as negative edges. When evaluating positive test recommendations against a pool of randomly sampled 100 non-recommended second-order friends, the model achieves a precision@1 of 72.5%. Matching Twitter’s “Who to Follow” interface which typically displays a slate of three recommendations, we evaluate precision@3, reaching 69.1%, while precision@10 equals 64.3%.

Unlike standard recommendation systems that predict user reactions to suggestions, our model predicts X’s recommendation pipeline outputs. This shift in objective—predicting model behavior rather than user behavior—explains our model’s strong performance relative to literature benchmarks (54). Overall, embeddings  $\Phi$  successfully predict X’s “Who to Follow” recommendations observed with our plug-in, indicating that studying the inferred embedding space provides a good approximation for Twitter’s internal representation of entities.

## Simulating sources of bias (reliability of the embedding)

Next, we conducted experiments to assess the robustness of our procedure against several possible sources of bias. Because our subsequent analysis relies on identifying directions in the embedding space through Canonical Correlation Analysis (CCA), we assess the robustness of learned embeddings up to non-singular affine transformations, as CCA is invariant to such transformations (55). We measure the average coefficient of determination  $R^2$  (56), as well as the average cosine similarity and inter-quantile value [2.5-97.5], between the reference embeddings  $\Phi$  of each user and each variant  $\tilde{\Phi}$  considered in different experiments, after applying the optimal nonsingular affine transformation determined through least squares optimization.

First, we conducted experiments assessing the stability of the embedding for different parameters determining the training. We performed 10 training runs using the original training dataset, saving the learned representations after 3, 5, and 10 epochs. Original embeddings were learned at 3 epochs, as determined optimal on the validation dataset. The coefficients of determination  $R^2$  between  $\Phi$  and  $\tilde{\Phi}$  show consistent stability across non-deterministic training runs, with highest values at 3 epochs ( $R^2 = 0.84759 \pm 0.00052$ ), and an average pairwise cosine similarity of 0.949 [0.873, 0.973]. Embedding stability decreases thereafter, with  $R^2$  values dropping at 5 epochs ( $R^2 = 0.83757 \pm 0.00062$ ) and 10 epochs ( $R^2 = 0.77506 \pm 0.00066$ ). We also compared embeddings for different values for  $\alpha$  in (1). We performed five training runs on the original training dataset for 3 epochs, setting  $\alpha$  to 42.6%, and 87.6% (the original embeddings  $\Phi$  were learned with  $\alpha = 62.6\%$ , optimal value on the validation dataset), achieving validation AUC-ROC scores of  $0.7503 \pm 0.0019$  and  $0.7494 \pm 0.0019$  respectively (standard deviation over ten replicates, and  $R^2$  between embeddings  $\Phi$  and variants  $\tilde{\Phi}$  of  $0.8417 \pm 0.0041$  for  $\alpha = 42.6\%$  and  $0.7762 \pm 0.0061$  for  $\alpha = 87.6\%$  (standard deviation over five replicates)). Complementarily, the average pairwise cosine similarity was 0.946 [0.856, 0.971] and 0.932 [0.822, 0.965]. See further details and additional experiments in SI Section C.2.2, including experiments with alternative positive-to-negative edge ratios, negative sampling strategies and degree threshold in the selection of users.

Second, we conducted experiments assessing the stability of the embedding against different socio-demographical compositions, and possible changes occurred in the platform during the observation period. Our browser plug-in only captures recommendations displayed on Twitter’s desktop interface. In our data, we observe that each account is suggested 5.11 times on average to the same volunteer. We thus postulate that most potentially missed recommendations for volunteers are redundant with desktop ones and thus already included in the training dataset, prompting us to experiment with different compositions of data using our observed recommendations. Assuming volunteers spend 50% of their X consumption on desktop browsers and 50% on other devices, we estimate that we may miss up to 19.6% of unique accounts recommended to volunteers. To simulate this effect, we augment each volunteer’s dataset by adding 19.6% of *artificial non-observed* positive edges, randomly sampled following the same rationale as for the previous curation of negative edges. We trained variant embeddings  $\tilde{\Phi}$  using identical hyperparameters as reference embeddings  $\Phi$  (3 epochs,  $\alpha = 62.6\%$ ) on 10 random samplings of additional “Who to Follow” edges. The average coefficient of determination  $R^2$  between embeddings  $\Phi$  and  $\tilde{\Phi}$  was  $0.8417 \pm 0.0033$ , and the average cosine similarity of 0.946 [0.855, 0.970]. In a more extreme scenario, where users spend 75% of their Twitter consumption on non-observed devices (meaning that we

would be missing potentially 39.2% of recommendations) the  $R^2$  between  $\Phi$  and 10 variants  $\tilde{\Phi}$  with 39.2% artificial non-observed positive edges remained high at  $0.8177 \pm 0.0031$ , and the average cosine similarity at 0.942 [0.840, 0.969].

In our study volunteers are self-selected. Upon enrollment, volunteers may indicate their age, gender, and political preference on a continuous scale from far-Left to far-Right (see Extended Figure S9), revealing that respondents tended to be Left-leaning males over 35 years old. To evaluate the impact of demographic skew, we constructed alternative training datasets of recommendations served only to subsets of volunteers who completed the survey. Using 3 epochs and  $\alpha = 62.6\%$  (as with the original embedding), we trained variant embeddings  $\tilde{\Phi}$  over the following three datasets: a) 284 self-identified male volunteers, b) 186 volunteers aged over 35, and c) 218 Left-leaning volunteers. The coefficient of determination  $R^2$  between  $\Phi$  and  $\tilde{\Phi}$  was 0.654 for dataset (a), 0.552 for (b), and 0.611 for (c). Similarly, the average pairwise cosine similarity was for dataset (a) 0.870 [0.698 0.934], for (b) 0.825 [0.599 0.917] and for (c) 0.852 [0.655 0.926].

Our dataset of recommendations spans a 16-month collection period, with varying collection rates (see Extended Figure S4). A notable increase in “Who to Follow” recommendations occurred in May 2023, around the time of policy changes on the platform. We hypothesize that these changes raised interest on the part of users to know more about the quality of the recommender, increasing the rate of volunteers, as they were offered personalized analyses. To assess potential effects of changes in population, we split the dataset into two periods: recommendations collected before and after May 1st, 2023. We then computed inferences of embeddings using our previously described methodology. The embeddings learned from these temporal splits show significant alignment with the original embeddings  $\Phi$ , achieving  $R^2$  values of 0.784 and 0.773 for the pre-May and post-May 2023 periods, respectively. The average cosine similarity was 0.921 [0.669 0.967] and 0.927 [0.726 0.968] respectively.

In our training dataset, we aggregated all accounts followed by volunteers, irrespective of when they started following them, with one notable exception: if a WTF suggestion turned into a friend, we solely considered the WTF observation, as the signal was scarcer for these cases. Consequently, some accounts in the training dataset labeled as “friends” were not followed when the first WTF recommendations were collected. Similarly, users in our sample might have unfriended/unfollowed some accounts included in our study. To assess how robust our embeddings  $\Phi$  are against these changes, we compared volunteers’ friends lists at the beginning and at the end of our observation period, allowing us to derive friend addition and removal rates. This revealed that, at most, 36.9% of friends in the training set were either a) not yet followed (26.7%) at the experiment’s start, or b) removed from the friend pool (10.2%) since then. We

thus randomly removed 36.9% of friends from the training dataset and computed the corresponding alternative embeddings  $\tilde{\Phi}$ , repeating this process three times. The comparison between  $\Phi$  and  $\tilde{\Phi}$  achieved a coefficient of determination  $R^2$  of  $0.80217 \pm 0.00028$  (standard deviation over three replicates), and an average cosine similarity of 0.931 [0.841 0.965]. See further details and additional experiments in SI Section C.2.3, including the removal of edges between several groups of users and training of embeddings using data from different time-periods

## Political attributes of users

We leverage a dataset of ideologically positioned X users developed by Ramaciotti et al. (57) to investigate representations of ideology in embeddings  $\Phi$ . This dataset contains 494 065 Twitter users interested in French politics, positioned along two political scales or dimensions: 1) a Left-Right ideology dimension and 2) a dimension measuring attitudes towards elites and institutions. The dataset comes with a detailed documentation (28) explaining the methodology used and the quality metrics showcasing the accuracy of inferred political positions.

The methodology relies on two steps. Step (1) uses ideological scaling (22) of follower networks, first developed for Liberal-Conservative ideological spatialization of Twitter users (3), and subsequently developed to capture additional political dimensions (4). The population in (57) is chosen among users that follow at least three Members of Parliament (MPs) on X/Twitter (as Barberà did in his 2015 studies (3, 29)), selecting 494 065 users that have an interest in national politics. Next, the follower network subtended by these users is collected, and a political homophily process is proposed as an explanation for the observed following links connecting MPs and their users:

$$P(U_i \rightarrow MP_j | \alpha_i, \beta_j, \gamma, \varphi_i, \varphi_j) = \text{logistic}(\alpha_i + \beta_j - \gamma \|\varphi_i - \varphi_j\|^2), \quad (3)$$

where,  $U_i \rightarrow MP_j$  stands for the event in which user  $U_i$  follows  $MP_j$ ,  $\alpha_i$  is the level of *activity* of user  $U_i$  measured in number of followed accounts,  $\beta_j$  is the level of *popularity* of  $MP_j$ , measured in number of followers,  $\gamma$  is a scale variable, and  $\varphi_i$  and  $\varphi_j$  are the multidimensional positions of  $U_i$  and  $MP_j$  in some unobservable multidimensional space. This data generation process is homophilic in the sense that  $P(U_i \rightarrow MP_j)$  increases as the distance between unobservable positions  $\|\varphi_i - \varphi_j\|$  in some latent space decreases. Step (1) involves using observed follower networks between MPs and their followers to infer the parameters of the model in (3). The reader is referred to the work of Barberà on Twitter (29) for the detailed methodology on this inference and to

the documentation of the dataset we use (28) for the details of the application of the methods to the data of this study.

Step (2) uses political survey data to calibrate multidimensional positions  $\varphi_i$  resulting from the Bayesian inference for the parameters of (3), as  $P(U_i \rightarrow MP_j)$  is invariant to isometries on positions  $\varphi_i$  and  $\varphi_j$ . For calibration and identification, the dataset from (28) uses party positions available for political parties, from the Chapel Hill Expert Survey (CHES) (30), created with the responses from hundreds of experts in political science, who position political parties along relevant dimensions. Creating proxies for party positions as the centroids of MPs  $\varphi_j$ , the dataset from (28) is compounded with an affine transformation going from the parameter space resulting from the Bayesian inference using (3), onto the space of the dimensions of the CHES data. The leading political dimension of the CHES data is the Left-Right dimension (ranging from 0 to 10, from Left to Right, for positions of parties). Because the scale used for calibration is constructed for positions of political parties, users can have positions to the left of position 0 (the leftmost position for parties) and to the right of position 10 (the rightmost position for parties). Previous research has shown that a second relevant dimension in France is the dimension measuring attitudes towards elites and institutions (58). Because of its importance and availability in the dataset we also leverage this second dimension in our study. Extended Figure S14 shows the density of users in the population along these two dimensions, and the positions of MPs and parties used for the calibration. Extended Figure S15 shows validations metrics proposed in (28) for positions of users along these two dimensions, based on annotations of profiles of users. See Section D.4 of the SI for a detail presentation of this dataset.

An analysis of this dataset reveals that 8 249 users in the population  $\mathcal{E}$  of our study (31.1%) also have political positions in the dataset from (28). Extended Figure S16 shows that the distributions of users from  $\mathcal{E}$  that have both, Left-Right and Anti-elite rhetoric positions do not deviate significantly from the French population delimited in the construction of the data set from (28).

## Estimating demographic attributes of users

We analyze profile pictures, screen names, usernames, and biographical descriptions to infer demographic attributes for users our study, applying the Multi-modal, Multilingual, and Multi-attribute (M3) model, developed by Wang et al. (23), on the 24 425 accounts in  $\mathcal{E}$  that have available information (see Extended Figure S11 for the gender and age distributions of profiles inferred by M3).

We assessed the accuracy of these inferences by comparing inferred age and gender with self-declared values (for volunteers), yielding an F1-score of 0.84 for gender and an average F1-score of 0.82 for the age groups. Section D.2 of the SI provides further details of this assessment, as well as

other forms of assessment, based on comparisons with inferences with a second mode (FairFace (59)), on analyses comparing inferred ages and dates of creations of accounts, and finally on analyses characterizing the most salient words used in posts by gender and age groups.

## Estimating additional attributes of users

We also established additional attributes of users: their popularity measured in number of followers (as this is probably relevant in recommendations), and the degree of interest of users in different topics. Interest in different topics discussed on X is known to be part of the features considered by the content (e.g., tweet) recommender system (41). We established the number of followers using metadata provided by the API for each user, ranging from 0 to 197 million among users in  $\mathcal{E}$ , with a median of 7 987. On 27th October 2024, we collected the last 200 tweets (published or retweeted) from 25 080 users in  $\mathcal{E}$  (excluding private and deleted accounts), totaling 2.3 million tweets. We leveraged the multi-topic classification model `cardiffnlp/tweet-topic-21-multi` developed by Antypas et al. (31) specifically conceived for tweets, to categorize each tweet into 19 generic topics including arts & culture, news & social concern, and science & technology. Non-English tweets were translated using Opus-MT model before topic inference. We measure the degree of interest of a user for a topic as the proportion of tweets per topic for each user across all 19 categories considered by (31). “News & Social Concern”, hereinafter simply *news*, is the most discussed topic among embedded users (Extended Figure S13 shows the distribution of interests in all topics). As we did with age groups, we report the 25 most overrepresented words in tweets classified under each topic, compared to their expected frequency under uniform random distribution across topics, showing that our metric captures interest in topics from (31) in our population (see Extended List S2).

Finally, we computed additional attributes of interest, including (see Extended Figure S10 for a full description): follower-to-friend ratio (assesses network reciprocity, with median 0.097), mean number of daily posts per user (as the total posts (status) divided by days since account creation, with median 2.21 posts per day) and mean number of daily likes (as the total likes divided by days since account creation, with median 1.40 likes per day). We also identified in X profiles whether users had the legacy *verification* status (i.e., the blue check-mark sign signaling whether the account is “authentic, notable, and active”), typically granted (at the time of our collection) to public figures, journalists, and influential organizations before the platform’s verification policy changes. Up to 30.1% of the accounts in  $\mathcal{E}$  were, as of early 2023, verified. We complete our attributes with an estimation of the linguistic complexity displayed by users in their posts, computed as the average word-length in posts (after pre-processing to remove non-linguistic elements such

as mentions, hashtags, emojis, URLs; see Extended List S3 for the 15 words with the highest frequency in the first and last decile of users according to the word-length metric).

## Measuring attributes encoded in the embedding space

Let us  $\Phi \in \mathbb{R}^{n \times d}$  denote the matrix of user embeddings, where each row  $\phi_u^\top \in \mathbb{R}^d$  represents the embedding vector of user  $u \in \{1, \dots, n\}$  in a  $d$ -dimensional embedding space; in our case  $d = 256$  and  $n = |\mathcal{E}| = 26,509$ . Given an attribute vector  $\mathbf{a} \in \mathbb{R}^n$ , where  $a_i$  corresponds to a measured characteristic of user  $i$  (political leaning, age, gender or any other of the inferred attributes), we aim to identify the direction in the embedding space such that projections along the direction that maximally correlate with this attribute.

For any unit vector  $\mathbf{w} \in \mathbb{R}^d$ , the correlation between the projection of user embeddings onto the direction spanned by  $\mathbf{w}$  and the attribute vector  $\mathbf{a}$  is given by:

$$\rho_{\mathbf{a}}^\Phi(\mathbf{w}) = \frac{(\Phi\mathbf{w})^\top \mathbf{a}}{\|\Phi\mathbf{w}\|_2 \|\mathbf{a}\|_2} \quad (4)$$

where  $\|\cdot\|_2$  denotes the Euclidean norm. We seek to find  $\mathbf{w}_\mathbf{a}$  such that the projection  $\Phi\mathbf{w}_\mathbf{a}$  of users' embeddings  $\Phi$  onto  $\mathbf{w}_\mathbf{a}$  maximally correlate with  $\mathbf{a}$ :

$$\mathbf{w}_\mathbf{a} = \underset{\mathbf{w} \in \mathbb{R}^d : \|\mathbf{w}\|_2=1}{\operatorname{argmax}} \rho_{\mathbf{a}}^\Phi(\mathbf{w}) \quad (5)$$

This optimization problem is a special case of Canonical Correlation Analysis (CCA), where one seeks to find a linear combination that maximizes correlation between a univariate dataset (the attribute vector  $\mathbf{a}$ ) and a multivariate dataset (the user embeddings  $\Phi$ ). The vector  $\mathbf{w}_\mathbf{a}$  can then be readily obtained by solving the CCA eigenvalue problem. To establish statistical significance of the identified directions, we employ a permutation test with  $N = 10^4$  repetitions. For each iteration, we generate  $\tilde{\mathbf{a}}$  by randomly permuting the elements of  $\mathbf{a}$ , compute  $\mathbf{w}_{\tilde{\mathbf{a}}}$  through CCA, and measure the resulting correlation  $\rho_{\tilde{\mathbf{a}}}^\Phi(\mathbf{w}_{\tilde{\mathbf{a}}})$ . By permuting the feature vector, we obtain the null distribution of correlations expected if the embedding space under consideration was not meaningfully encoding the feature of interest. The one-sided p-value is subsequently determined as the proportion of permuted absolute correlations that exceed the absolute observed correlation  $\rho_{\mathbf{a}}^\Phi(\mathbf{w}_\mathbf{a})$ .

Figure 3. A shows the Pearson correlation induced by the CCA directions capturing the main attributes in our study (all p-values  $< 0.0001$ ). Extended Table S2 shows the Pearson correlation for all attributes estimated for our study.

## Validating directions in the embedding capturing attributes

After identifying through CCA the directions in the embedding space that induce positions that maximally correlates

with relevant attributes, we conduct additional validations showing that these CCA directions capture attributes. This is needed because of two reasons. 1) Even if a direction produces a high correlation in ordering and positioning users according to attributes for users, the variance or disturbance error of an underlying linear model might still be high. 2) Secondly, not every user in  $\mathcal{E}$  has known values for all attributes. Accordingly, we need to control that the CCA directions induce and ordering of users also for those that have no known attributes. The CCA direction for Left-Right leanings was computed relying on the 8 249 users from  $\mathcal{E}$  (31.1%) that had a position on the Left-Right scale, and we need to control that the direction orders the rest of users in  $\mathcal{E}$  correctly. To validate the positions on CCA directions independently from the data we used inferring a direction  $\mathbf{w}_\mathbf{a}$ , we analyze the friends and tweet content of users at both extremes of the direction. Specifically, we identify overrepresented friends (followed accounts), words, and hashtags in the tweets produced by users in the first and last deciles of positions along  $\mathbf{w}_\mathbf{a}$ . We determine overrepresented entities by comparing their observed frequency in the target pool to their expected frequency under uniform random distribution along the  $\mathbf{w}_\mathbf{a}$  direction. To protect privacy of users, we only included followed accounts with more than 50K followers and followed by at least 10% of the users in the considered decile. Section F of the SI shows the results of these validations for identified directions in the embedding capturing ideology, age, gender, and thematic interests among other attributes.

## Measuring the alignment between directions in the embedding

The measurements of alignment and dependence between positions along CCA directions presented in the article include Spearman correlations (Extended Figure S29) and cosine similarities in Figure 3.B. To assess the statistical significance of cosine similarities, we draw values of cosine similarities under a null hypothesis. Since the null distribution of attribute directions  $\mathbf{w}_\mathbf{a}$  depends on the distribution of user embeddings in  $\mathbb{R}^d$ , we use permutation tests, rather than assuming a uniform hyper-sphere distribution, to assess the significance of similarities between  $\mathbf{w}_\mathbf{a}$  and  $\mathbf{w}_\mathbf{b}$ , the embedding directions associated with features  $\mathbf{a}$  and  $\mathbf{b}$ . The one-sided p-value is computed as the proportion of randomized cosine similarities that exceed the observed similarity between  $\mathbf{w}_\mathbf{a}$  and  $\mathbf{w}_\mathbf{b}$ , where the randomized similarities are computed between embedding directions  $\mathbf{w}_{\tilde{\mathbf{a}}}$  and  $\mathbf{w}_{\tilde{\mathbf{b}}}$  associated with shuffled features  $\tilde{\mathbf{a}}$  and  $\tilde{\mathbf{b}}$ .

## Computing politically-constrained recommendations

The method proposed for constraining the amount of information on political preferences of users available to the

recommender borrows from the method called “debiasing” by Bolukbasi et al. (35) for language models. We adapt this methodology to “protect” (34) user attributes from being used by recommender systems. Consider a user attribute  $\mathbf{a}$  to be protected. Using CCA, we first identify the direction  $\mathbf{w}_a$  for which the projection of positions of users in the embedding, i.e.,  $\Phi \mathbf{w}_a$ , maximally correlates with  $\mathbf{a}$ . We then project embedded positions of users  $\Phi$  onto  $\mathbf{w}_a^\perp$ , the subspace orthogonal to  $\mathbf{w}_a$ , removing linearly-encoded information about  $\mathbf{a}$  along this direction. In high-dimensional spaces, attributes may be potentially encoded in multiple orthogonal directions (36). Therefore, we repeat this process, iteratively reducing the effective dimension of the embedding, identifying each time the quality of the correlation achieved by the new CCA direction, until no spatial direction in the embedding induces a significant correlation with the attribute selected to be constrained or protected. For our experiment, we seek to protect Left-Right leanings of users, and we set the threshold of significance at 0.01, meaning that we consider that no further linear encoded is significant when the p-value of the correlation overflows above this value; corresponding to Pearson correlation of 0.19408, according to the distribution obtained through permutation. Importantly, this procedure only removes linearly-encoded information. However, since user recommendations are formulated through inner products between user embeddings, our procedure effectively constrains recommendations from leveraging attribute  $\mathbf{a}$ .

## Evaluating politically-constrained recommendations

Holding out 10% of observed WTF recommendations for evaluation, we find that the protected embeddings are 20.6% less informative (in terms of normalized mutual information) about whether a given recommendation was served to a user compared to the original (unprotected) embeddings. Subsequently, we use this protected embedding to compute friend recommendations to characterize relevant properties: relevance and accuracy of recommendations. To compute friend recommendations for each user  $s \in \mathcal{E}$ , we first select all users  $t \in \mathcal{E}$  that  $s$  does not already follow, and rank each potential recommendation (i.e., of user  $t$  to user  $s$ ) by evaluating the TransE scoring function (51):  $f(s, \text{WTF}, t) = (\phi_s + \varphi_{\text{WTF}})^T \phi_t$ , where  $\varphi_{\text{WTF}}$  represents the WTF relation embedding computed during training.

We measure the ideological diversity of friend recommendations made to each user as the standard deviation of the Left-Right position of the recommended friends. To measure thematic relevance of recommendations, we inspect the relative interest in news content that recommended friends have when compared to the users receiving recommendations (among types of contents, news content is both relevant and in risk of being affected by signals re-

lated ideological leaning). Interest in news content is measured as the fraction of tweets published or shared that were classified as related to “News & Social Concern” by the `cardiffnlp/tweet-topic-21-multi`. For each user we measure the mean distance between its own interest in news and those of proposed recommendations. Figure 4 reports results based on 50 recommendations per user  $s$ . Extended Figure S31 shows the effect of the protected embedding on the diversity of recommendations for users separated into three groups according to ideological leaning: Left-leaning (ideological leaning below 4.5), Center-leaning (ideological leaning between 4.5 and 7), and Right-leaning users (ideological leaning above 7).

## References

1. A. Amini, A. P. Soleimany, W. Schwarting, S. N. Bhattacharya, D. Rus, Uncovering and mitigating algorithmic bias through learned latent structure, in *Proceedings of the 2019 AAAI/ACM Conference on AI, Ethics, and Society* (2019), pp. 289–295.
2. T. Fagni, S. Cresci, Fine-grained prediction of political leaning on social media with unsupervised deep learning. *Journal of Artificial Intelligence Research* **73**, 633–672 (2022).
3. P. Barberá, Birds of the same feather tweet together: Bayesian ideal point estimation using Twitter data. *Political analysis* **23** (1), 76–91 (2015).
4. P. Ramaciotti, et al., Inferring attitudinal spaces in social networks. *Social Network Analysis and Mining* **13** (1), 14 (2022).
5. P. Lorenz-Spreen, L. Oswald, S. Lewandowsky, R. Hertwig, A systematic review of worldwide causal and correlational evidence on digital media and democracy. *Nature human behaviour* **7** (1), 74–101 (2023).
6. E. Bakshy, S. Messing, L. A. Adamic, Exposure to ideologically diverse news and opinion on Facebook. *Science* **348** (6239), 1130–1132 (2015).
7. P. Bouchaud, D. Chavaliarias, M. Panahi, Crowd-sourced audit of Twitter’s recommender systems. *Scientific Reports* **13** (1) (2023), doi:10.1038/s41598-023-43980-4, <http://dx.doi.org/10.1038/s41598-023-43980-4>.
8. S. Milli, et al., Engagement, user satisfaction, and the amplification of divisive content on social media. *PNAS nexus* **4** (3), pgaf062 (2025).
9. K. Duskin, J. S. Schafer, J. D. West, E. S. Spiro, Echo Chambers in the Age of Algorithms: An Audit of Twitter’s Friend Recommender System, in *ACM Web Science*

- Conference, Websci '24 (ACM) (2024), p. 11–21, doi: 10.1145/3614419.3643996.
10. B. Nyhan, *et al.*, Like-minded sources on Facebook are prevalent but not polarizing. *Nature* **620** (7972), 137–144 (2023).
  11. F. Huszár, *et al.*, Algorithmic amplification of politics on Twitter. *Proceedings of the National Academy of Sciences* **119** (1), e2025334119 (2022).
  12. C. Jia, M. S. Lam, M. C. Mai, J. T. Hancock, M. S. Bernstein, Embedding Democratic Values into Social Media AIs via Societal Objective Functions. *Proceedings of the ACM on Human-Computer Interaction* **8** (CSCW1), 1–36 (2024), doi:10.1145/3641002, <http://dx.doi.org/10.1145/3641002>.
  13. L. Rheault, C. Cochrane, Word embeddings for the analysis of ideological placement in parliamentary corpora. *Political analysis* **28** (1), 112–133 (2020).
  14. J. Milbauer, A. Mathew, J. Evans, Aligning multidimensional worldviews and discovering ideological differences, in *Proceedings of the 2021 conference on empirical methods in Natural Language Processing* (2021).
  15. T. Faverjon, P. Ramaciotti, Discovering ideological structures in representation learning spaces in recommender systems on social media data, in *Proceedings of the International Conference on Advances in Social Networks Analysis and Mining* (2023), pp. 400–406.
  16. C. Sandvig, K. Hamilton, K. Karahalios, C. Langbort, Auditing algorithms: Research methods for detecting discrimination on internet platforms. *Data and discrimination: converting critical concerns into productive inquiry* **22** (2014), 4349–4357 (2014).
  17. L. Van Vliet, P. Törnberg, J. Uitermark, The Twitter parliamentarian database: Analyzing Twitter politics across 26 countries. *PLoS one* **15** (9), e0237073 (2020).
  18. A. Jungherr, Twitter use in election campaigns: A systematic literature review. *Journal of information technology & politics* **13** (1), 72–91 (2016).
  19. H. Kwak, C. Lee, H. Park, S. Moon, What is Twitter, a social network or a news media?, in *Proceedings of the 19th international conference on World wide web* (2010), pp. 591–600.
  20. Twitter, Twitter's Recommendation Algorithm, [https://blog.x.com/engineering/en\\_us/topics/open-source/2023/twitter-recommendation-algorithm](https://blog.x.com/engineering/en_us/topics/open-source/2023/twitter-recommendation-algorithm), accessed: 2024-12-29.
  21. A. El-Kishky, *et al.*, Twhin: Embedding the twitter heterogeneous information network for personalized recommendation, in *Proceedings of the 28th ACM SIGKDD conference on knowledge discovery and data mining* (2022), pp. 2842–2850.
  22. J. Clinton, S. Jackman, D. Rivers, The statistical analysis of roll call data. *American Political Science Review* **98** (2), 355–370 (2004).
  23. Z. Wang, *et al.*, Demographic inference and representative population estimates from multilingual social media data, in *The world wide web conference* (2019), pp. 2056–2067.
  24. Twitter, Discovering Who To Follow, [https://blog.x.com/official/en\\_us/a/2010/discovering-who-to-follow.html](https://blog.x.com/official/en_us/a/2010/discovering-who-to-follow.html), accessed: 2025-01-06.
  25. A. Goel, *et al.*, The who-to-follow system at Twitter: strategy, algorithms, and revenue impact. *Interfaces* **45** (1), 98–107 (2015).
  26. Twitter, Twitter/The-Algorithm/Twitter's Recommendation Algorithm, <https://github.com/twitter/the-algorithm/tree/main> (2023).
  27. X. Zhang, *et al.*, Twhin-bert: A socially-enriched pre-trained language model for multilingual tweet representations at twitter, in *Proceedings of the 29th ACM SIGKDD conference on knowledge discovery and data mining* (2023), pp. 5597–5607.
  28. P. Ramaciotti, J. Royo-Letelier, J.-P. Cointet, A. Pournaki, Attitudinally-positioned European sample dataset. *Social Media for Democracy, Sciences Po Paris* p. 18 p. (2024).
  29. P. Barberá, J. T. Jost, J. Nagler, J. A. Tucker, R. Bonneau, Tweeting from left to right: Is online political communication more than an echo chamber? *Psychological science* **26** (10), 1531–1542 (2015).
  30. S. Jolly, *et al.*, Chapel Hill Expert Survey trend file, 1999–2019. *Electoral Studies* **75**, 102420 (2022), doi:10.1016/j.electstud.2021.102420, <http://dx.doi.org/10.1016/j.electstud.2021.102420>.
  31. D. Antypas, *et al.*, Twitter Topic Classification, in *Proceedings of the 29th International Conference on Computational Linguistics* (International Committee on Computational Linguistics, Gyeongju, Republic of Korea) (2022), pp. 3386–3400.
  32. G. Ivaldi, Populism in France, in *Populism Around the World. A Comparative Perspective*, D. Stockemer, Ed. (Springer), pp. 27–48 (2018), doi:10.1007/978-3-319-96758-5\\_3, <https://shs.hal.science/halshs-01889832>.

33. X. He, P. Niyogi, Locality Preserving Projections, in *Advances in Neural Information Processing Systems*, S. Thrun, L. Saul, B. Schölkopf, Eds. (MIT Press), vol. 16 (2003).
34. S. Ravfogel, Y. Elazar, H. Gonen, M. Twiton, Y. Goldberg, Null It Out: Guarding Protected Attributes by Iterative Nullspace Projection, in *Proceedings of the 58th Annual Meeting of the Association for Computational Linguistics*, D. Jurafsky, J. Chai, N. Schluter, J. Tetreault, Eds. (Association for Computational Linguistics, Online) (2020), pp. 7237–7256, doi:10.18653/v1/2020.acl-main.647.
35. T. Bolukbasi, K.-W. Chang, J. Y. Zou, V. Saligrama, A. T. Kalai, Man is to Computer Programmer as Woman is to Homemaker? Debiasing Word Embeddings, in *Advances in Neural Information Processing Systems*, D. Lee, M. Sugiyama, U. Luxburg, I. Guyon, R. Garnett, Eds. (Curran Associates, Inc.), vol. 29 (2016).
36. H. Gonen, Y. Goldberg, Lipstick on a Pig: Debiasing Methods Cover up Systematic Gender Biases in Word Embeddings But do not Remove Them, in *Proceedings of the 2019 Workshop on Widening NLP*, A. Axelson, D. Yang, R. Cunha, S. Shaikh, Z. Waseem, Eds. (Association for Computational Linguistics, Florence, Italy) (2019), pp. 60–63, <https://aclanthology.org/W19-3621>.
37. C. A. Bail, *et al.*, Exposure to opposing views on social media can increase political polarization. *Proceedings of the National Academy of Sciences* **115** (37), 9216–9221 (2018).
38. T. Mikolov, I. Sutskever, K. Chen, G. S. Corrado, J. Dean, Distributed representations of words and phrases and their compositionality. *Advances in neural information processing systems* **26** (2013).
39. S. Arora, Y. Li, Y. Liang, T. Ma, A. Risteski, A latent variable model approach to pmi-based word embeddings. *Transactions of the Association for Computational Linguistics* **4**, 385–399 (2016).
40. N. Elhage, *et al.*, Toy models of superposition. *arXiv preprint arXiv:2209.10652* (2022).
41. V. Satuluri, *et al.*, Simclusters: Community-based representations for heterogeneous recommendations at twitter, in *Proceedings of the 26th ACM SIGKDD international conference on knowledge discovery & data mining* (2020), pp. 3183–3193.
42. R. Xenidis, Beyond bias: algorithmic machines, discrimination law and the analogy trap. *Transnational Legal Theory* **14** (4), 378–412 (2023).
43. P. Ramaciotti, Depolarizing And Moderating Social Media With AI: Tools and guidelines leveraging representation spaces. *AI4Democracy, IE Center for the Governance of Change* (2024).
44. L. Grozdanovski, In search of effectiveness and fairness in proving algorithmic discrimination in EU law. *Common Market Law Review* **58** (1) (2021).
45. J. Strycharz, C. Meppelink, B. Zarouali, T. Araujo, H. Voorveld, The blind spot in data donations: who is (not) willing to donate digital data in social scientific research. *Computational Communication Research* **6** (2), 1 (2024).
46. Z. Kmetty, *et al.*, Determinants of willingness to donate data from social media platforms. *Information, Communication & Society* **28** (7), 1324–1349 (2025).
47. Z. Kmetty, *et al.*, Determinants of willingness to donate data from social media platforms in the US and Hungary. *Information, Communication & Society* **28** (7), 1324–1349 (2025).
48. A. Lerer, *et al.*, PyTorch-BigGraph: A Large-scale Graph Embedding System (2019), <https://arxiv.org/abs/1903.12287>.
49. E. Colleoni, A. Rozza, A. Arvidsson, Echo chamber or public sphere? Predicting political orientation and measuring political homophily in Twitter using big data. *Journal of communication* **64** (2), 317–332 (2014).
50. Y. Halberstam, B. Knight, Homophily, group size, and the diffusion of political information in social networks: Evidence from Twitter. *Journal of public economics* **143**, 73–88 (2016).
51. A. Bordes, N. Usunier, A. Garcia-Duran, J. Weston, O. Yakhnenko, Translating Embeddings for Modeling Multi-relational Data, in *Advances in Neural Information Processing Systems*, C. Burges, L. Bottou, M. Welling, Z. Ghahramani, K. Weinberger, Eds. (Curran Associates, Inc.), vol. 26 (2013).
52. X. Glorot, Y. Bengio, Understanding the difficulty of training deep feedforward neural networks, in *Proceedings of the Thirteenth International Conference on Artificial Intelligence and Statistics*, Y. W. Teh, M. Titterington, Eds. (PMLR, Chia Laguna Resort, Sardinia, Italy), vol. 9 of *Proceedings of Machine Learning Research* (2010), pp. 249–256, <https://proceedings.mlr.press/v9/glorot10a.html>.
53. J. Duchi, E. Hazan, Y. Singer, Adaptive Subgradient Methods for Online Learning and Stochastic Optimization. *Journal of Machine Learning Research* **12** (61), 2121–2159 (2011), <http://jmlr.org/papers/v12/duchi11a.html>.

54. W. Hu, *et al.*, Open graph benchmark: datasets for machine learning on graphs, in *Proceedings of the 34th International Conference on Neural Information Processing Systems*, NIPS '20 (Curran Associates Inc., Red Hook, NY, USA) (2020).
55. A. Mathai, S. Provost, H. Haubold, *Chapter 10: Canonical Correlation Analysis* (Springer International Publishing), p. 641–677 (2022), doi:10.1007/978-3-030-95864-0\_10.
56. D. Stewart, W. Love, A general canonical correlation index. *Psychological bulletin* **70** (3p1), 160 (1968).
57. P. Ramaciotti, J. Royo-Leterier, J.-P. Cointet, A. Pournaki, Attitudinally-positioned European sample dataset, <https://doi.org/10.6084/m9.figshare.25288210.v1> (2024).
58. P. Ramaciotti, J.-P. Cointet, G. M. Zolotoochin, Unfolding the dimensionality structure of social networks in ideological embeddings, in *Proceedings of the 2021 IEEE/ACM international conference on advances in social networks analysis and mining* (2021), pp. 333–338.
59. K. Karkkainen, J. Joo, FairFace: Face Attribute Dataset for Balanced Race, Gender, and Age for Bias Measurement and Mitigation, in *2021 IEEE Winter Conference on Applications of Computer Vision (WACV)* (IEEE) (2021), p. 1547–1557, doi:10.1109/wacv48630.2021.00159.

## Acknowledgments

This work has been partially funded by the “European Polarisation Observatory” (EPO) of CIVICA Research (co-)funded by EU’s Horizon 2020 programme under grant agreement No 101017201, by European Union Horizon program project “Social Media for Democracy” under grant agreement No 101094752 ([www.some4dem.eu](http://www.some4dem.eu)), by the *Very Large Research Infrastructure* (TGIR) Huma-Num of CNRS, Aix-Marseille Université and Campus Condorcet, and by Project Liberty Institute project “AI-Political Machines” (AIPM). P.B. acknowledges financial support from the CFM Foundation for sciences.

## Supplementary Information

Check the article version with the Supplementary Information at:

<https://hal.science/hal-05468493v1/document>.